

Flat-band many-body localization in the Creutz ladder

Yoshihito Kuno*

Department of Physics, Graduate School of Science, Kyoto University, Kyoto 606-8502, Japan

Takahiro Orito* and Ikuo Ichinose

Department of Applied Physics, Nagoya Institute of Technology, Nagoya, 466-8555, Japan

(Dated: April 9, 2019)

Study on disorder-free many-body localization is reported for the flat-band Creutz ladder, which was recently realized in cold-atoms in an optical lattice. In non-interacting case, the flat-band structure leads to a Wannier wave function localized on four adjacent lattice sites. In the flat-band regime with and without interactions, level spacing analysis exhibits Poisson-like distribution. This indicates the existence of the disorder-free localization. Calculation of the inverse participation ratio supports this observation. Interestingly, this type of localization is robust against weak disorder, and then for strong disorder, the system exhibits a crossover into the ordinary many-body localization phase. We also find non-ergodic dynamics in the flat-band regime without disorder. Memory of an initial density-wave pattern is preserved for a long period.

Introduction.— Localization and absence of diffusion in non-interacting electron systems have been extensively studied since Anderson discussed disorder effect on single particle electron wavefunction in solid [1]. Today what is called, Anderson localization (AL) is recognized as a universal phenomenon in various physical systems [2]. In AL quantum systems, single particle electron wavefunction is exponentially localized with a localization length, which leads to a kind of insulating phase. Thanks to recent development of both computer power and numerical techniques, study on effect of interactions between particles on the AL is one of the main research topics in condensed matter physics nowadays. It is now recognized that AL survives in some cases even if interactions between particles exist. This is so-called many-body localization (MBL). Mostly by using numerical simulations, it has been clarified that the MBL phase exhibits some characteristic properties such as Poisson distribution in the level spacing analysis (LSA) of energy eigenvalues similar to that of the ordinary AL and logarithmic growth of entanglement entropy. In its galssy dynamics, MBL is closely related with breaking of eigenstate thermalization hypothesis, and ergodicity breaking dynamics [3–7]. Recent experiments on cold-atom gases in optical lattices have reported evidences for the existence of the MBL phenomena [8, 9].

Until recently, most of the theoretical studies have focused on possible MBL induced by disorders encoded in on-site potentials, hopping amplitudes and interactions, as well as a quasi-periodic potential [10]. On the other hand very recently, disorder-free AL/MBL-like phenomena have been discovered in the Wannier-Stark ladder [11, 12], dipolar-atom gases in an optical lattice [13], some lattice-gauge theoretical models [14–17] and quantum Hall system [18]. Motivated by these discoveries, we shall report another type of disorder-free MBL system in this letter. It is a flat band system with interactions. The flat band structure suppresses particle hopping ef-

fectively and generates a localized Wannier state [19, 20] similar to the typical localized wavefunction in the ordinary AL system. We are inspired by the existence of such localized wave functions and study the flat-band type localization in the Creutz ladder [21]. The Creutz ladder is a simple model and is also experimentally feasible in cold-atom gases [22–24]. We investigate the LSA with weak disorders under the flat band condition, and find that the probability distribution exhibits Poissonian behavior for both the non-interacting and interacting cases, indicating localization tendency. Inverse participation ration (IPR) supports the localization tendency as well. Furthermore, we find that the dynamics in the flat-band Creutz ladder exhibits ergodicity breaking dynamics, i.e., memory of particle distribution in initial states survives for a long time period.

Creutz ladder model.— In this work, we study an interacting Creutz ladder with the Hamiltonian [21],

$$\begin{aligned} H = & \sum_j \left[-it_1(a_{j+1}^\dagger a_j - b_{j+1}^\dagger b_j) - t_0(a_{j+1}^\dagger b_j + b_{j+1}^\dagger a_j) + \text{h.c.} \right. \\ & + V(n_{a,j}n_{a,j+1} + n_{b,j}n_{b,j+1} + n_{a,j}n_{b,j+1} + n_{b,j}n_{a,j+1}) \\ & \left. + \mu_{a,j}n_{a,j} + \mu_{b,j}n_{b,j} \right], \end{aligned} \quad (1)$$

where $a_j^{(\dagger)}$ and $b_j^{(\dagger)}$ are fermion annihilation (creation) operators on the upper and lower chains, respectively, and subscript j denotes a unit cell. $n_{a(b),j}$ is the number operator of the particle on the upper (lower) chain. t_1 and t_0 are the intra-chain and inter-chain hopping amplitudes, respectively. V is the intra-chain and inter-chain repulsions as depicted in Fig. 1 (a). $\mu_{a(b),j}$ is random disorder chemical potential, which has a uniform distribution such as $\mu_{a(b),j} \in [-\mu/2, \mu/2]$. The model is feasible in recent experiments by using a synthetic dimensional method [22, 23] or spin-dependent lattice with lattice modulation technique [24].

The energy spectrum of the non-interacting case of

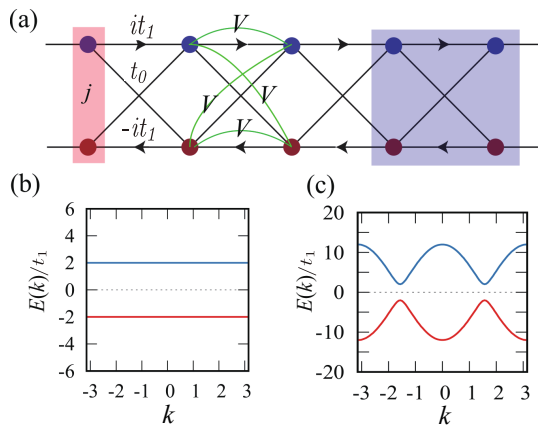


FIG. 1: (a) Creutz ladder: the red shaded area represents a unit cell and the blue one is a Wannier state for the flat-band condition $t_1 = t_0$. (b) Flat-band structure at $t_1 = t_0$. (c) Dispersive (non-flat-band) band structure at $t_1 = 6t_0$.

H in Eq. (1) with $V = \mu = 0$ is given as $E(k) = \pm\sqrt{(2t_1 \sin k)^2 + (2t_0 \cos k)^2}$, where k is the wave number and the band width is $|2(t_1 - t_0)|$. As shown in Figs. 1 (b) and (c), the band is flat for $t_1 = t_0$ with $E(k) = -2t_1$, while for $t_1 \neq t_0$ the band is dispersive. The non-interacting case of H in Eq. (1) with $\mu = 0$ belongs to the BDI or AIII class in the topological classification theory [25, 26]. This symmetry affects the spectrum distribution of the system. In particular, the chiral symmetry makes the energy spectrum symmetric around the zero energy. Also, at the flat band point $t_0 = t_1$, a localized Wannier state exists in the system, whose wave function is given by [19, 20]

$$|\Psi_w\rangle = -\frac{1}{2} \left[i a_j^\dagger + a_{j+1}^\dagger + b_j^\dagger + i b_{j+1}^\dagger \right] |0\rangle, \quad (2)$$

where $|0\rangle$ is the vacuum state. This state spans over two adjacent unit cells, that is, a four-site localized state. As we show, this state is a key ingredient for appearance of a new kind of localization.

Here we note that in the ordinary AL, disorder makes localized states substantially reside on a *single lattice site*. On the other hand in the flat-band case, the target Wannier state has finite components in a finite region with *multiple lattice sites*. In the Creutz ladder case, the number of site is four as shown in Eq. (2). [See also Fig. 1 (a).] As we explain later on, this fact gives certain constraints on the setup of an initial state for observing MBL dynamics.

Level spacing analysis and IPR.— In order to investigate localization properties of the present model, we first study the LSA by full-diagonalizing the Hamiltonian H in Eq.(1) with the periodic boundary condition. In the LSA, we employ the usual unfolding analysis [27] in order to obtain a clear probability distribution of the level

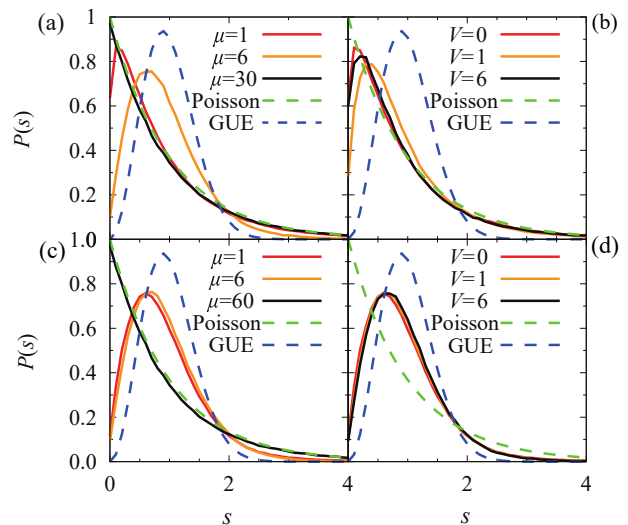


FIG. 2: Level spacing analysis: (a) Disorder dependence in non-interacting flat-band ($V = 0$). (b) Interaction dependence in disordered flat-band ($\mu = 1$). (c) Disorder dependence in non-interacting non-flat-band ($V = 0$). (d) Interaction dependence in disordered non-flat-band ($\mu = 1$).

spacings of energy eigenvalues. Here, our interest is the disorder-free and weak disorder regimes. On performing the LSA for disorder-free case ($\mu = 0$), it is important to notice that the system has the translational symmetry. This symmetry generally leads to many degeneracies in energy eigenvalues. Because of the degeneracies, it is not straightforward to identify probability distributions of the level spacings without ambiguities [11, 12]. In order to avoid this difficulty, we consider the cases with small but finite disorders. In the presence of disorders, even if they are very weak, the degeneracies of the energy eigenvalues are solved, and then we are able to obtain clear probability distribution of level spacings, which substantially captures the characteristics of the disorder-free system. In practical calculations, we consider the upper and lower chains with length $L = 16$ and the number of particle N is four (i.e., filling factor is $1/8$). The Hilbert space dimension expanded by the Fock state is 35960, and we discard the top and bottom 10% of the energy eigenvalues to obtain a clear distribution. From the LSA, we examine localization properties of the system. In general for an ensemble of localized states, the probability distribution exhibits Poisson statistics such as $P_P(s) \propto \exp(-s)$, where s denotes the unfolded level spacing. On the other hand for an ensemble of delocalized (extended) states, the probability distribution is to be Gaussian unitary ensemble (GUE) such as $P_G(s) \propto s^c \exp(-ds^2/\pi)$ with certain numbers c and d [6, 7, 28–35].

Figure 2 (a) shows the obtained probability distribution for various disorder strengths for the non-interacting flat-band ($V = 0, t_1 = t_0$). We find that for the weak dis-

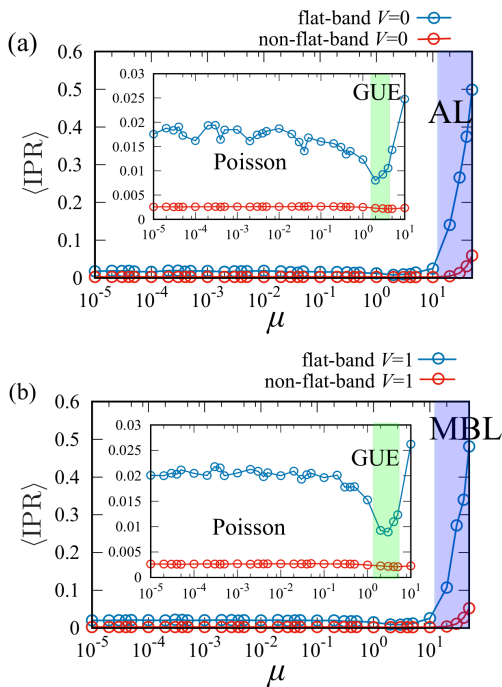


FIG. 3: Disorder dependence of the averaged IPR: (a) Non-interacting case ($V = 0$). (b) Interacting case ($V = 1$). For both cases, we averaged over 20 disorder samples. In weak-disorder regime ($\mu < 1$), there exists a large difference between the flat band and non-flat band in the value of the IPR. In both cases (a) and (b), the difference becomes small for $1 \lesssim \mu \lesssim 10$, where the LSA of the flat band exhibits the GUE-like distribution. In the $\mu \gtrsim 10$ regime, the averaged IPR grows rapidly. This indicates existence of a crossover to the disorder-induced AL or MBL phase. The system size is $L = 12$ and the particle number $N = 3$.

order ($\mu = 1$), the probability distribution is very close to Poisson statistics. This result indicates the existence of localized states even in the weak disorder as it is expected. As increasing the disorder strength, we observed an interesting phenomenon, i.e., the statistics changes from Poisson to GUE-like one first, and then it return to Poisson statistics. Calculations for $\mu = 6$ and $\mu = 30$ in Fig. 2 (a) clearly exhibit this behavior; Poisson \rightarrow GUE \rightarrow Poisson. The above behavior of the Creutz ladder model is somewhat different from the flat-band models studied in Refs. [33, 34]. We understand our findings as follows; The Poisson statistics for the $\mu = 30$ ensemble comes from the ordinary AL, which is induced by disorder. On the other hand, the origin of the Poisson-like statistics for the $\mu = 1$ ensemble is the flat-band properties of the model. Crossover takes place from the flat-band localization to the disorder-induced AL as disorder is increased [36]. This conclusion is supported by the inverse participation ration (IPR) calculated later on.

Figure 2 (b) shows the LSA of the interacting cases with weak disorder $\mu = 1$. We find that even for finite

interaction $V = 1$ and 6, Poisson-like statistics survives. This result implies the disorder-free MBL, which is induced by the flat-band structure.

We also study the non-flat-band case ($t = 6t_0$), which we regard a reference system with respect to the AL in finite-size systems. Figure. 2 (c) shows the LSA of the non-interacting non-flat-band for various μ 's. The $\mu = 1$ and $\mu = 6$ results are close to GUE, while for larger disorder $\mu = 60$, the ordinary disorder-induced AL appears. This delocalization-like behavior is stable against the interaction as shown in Fig. 2 (d). The obtained result, in particular for the non-interacting case, seems to contradict the common brief that all states are localized in 1D random-potential systems. Probably, this is a finite-size effect [37], i.e., localization lengths of certain part of states are larger than the system size for the weak disorder $\mu = 1$. By comparing results in Fig. 2 (a), (b) with those in Fig. 2 (c), (d), we find that localization in the flat-band is stronger than that in the non-flat-band, indicating that their mechanisms are different. We shall confirm this expectation by calculating other quantities.

We calculate the IPR, which is often used for study of localization. By diagonalizing the Hamiltonian of Eq. (1), we obtain all eigenvectors $|\psi_\ell\rangle = \sum_m c_m^\ell |F_m\rangle$, where ℓ labels eigenstates, $|F_m\rangle$ is the Fock state base and $\{c_m^\ell\}$ are coefficients. For these eigenstates, the IPR is defined by

$$(\text{IPR})_\ell = \sum_m |c_m^\ell|^4. \quad (3)$$

In particular for a non-interacting system with N particles, $(\text{IPR})_\ell$ in Eq. (3) is related to the localization length R_ℓ [in unit of the lattice spacing] as $(\text{IPR})_\ell \simeq 1/(R_\ell)^N$ [17]. In this work, we average $(\text{IPR})_\ell$ over all states for fixed μ and V . The averaged IPR is denoted by $\langle \text{IPR} \rangle$.

Figure 3 (a) shows the μ -dependence of $\langle \text{IPR} \rangle$ in non-interacting case ($V = 0$). For sufficiently weak disorder ($\mu \lesssim 1$), the obtained $\langle \text{IPR} \rangle$ in both the flat-band ($t_0 = t_1$) and non-flat band ($t_0 = 6t_1$) are small compared with the strong-disorder regime ($\mu \gtrsim 10$), where the value of $\langle \text{IPR} \rangle$ is large due to the ordinary AL. For the weak-disorder regime, there exists clear difference in $\langle \text{IPR} \rangle$ between the flat-band and the non-flat-band [38], i.e., the value of $\langle \text{IPR} \rangle$ of the flat-band is obviously much larger than that of the non-flat-band as shown in the inset of Fig. 3 (a). This means that the flat-band system is more localized than the non-flat-band system. Simple estimation of average of R_ℓ , $\langle R \rangle$, by using $\langle \text{IPR} \rangle$ gives $\langle R \rangle \simeq 8$ for the non-flat-band, whereas $\langle R \rangle \simeq 4$ for the flat-band. This result for the flat-band, $\langle R \rangle \simeq 4$, is reminiscent of the Wannier state in Eq. (2).

It is interesting to observe that in the vicinity $\mu \sim 6$, $\langle \text{IPR} \rangle$ decreases in the flat-band system as shown in the inset of Fig. 3 (a). This behavior is in good agreement with the result of LSA in Fig. 2 (a). In fact for $\mu = 6$, the

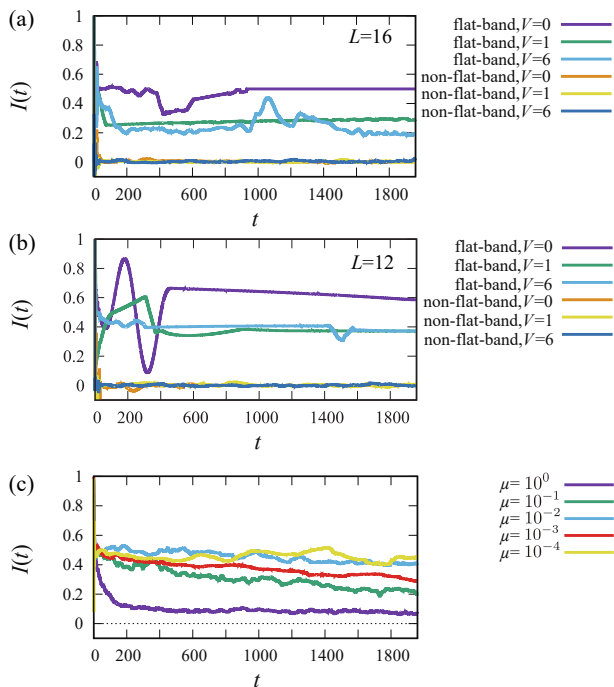


FIG. 4: Time evolution of Imbalance $I(t)$: (a) $L = 16$ disorder-free case. (b) $L = 12$ disorder-free case. (c) Disorder dependence for interacting flat-band case ($V = 1$). We averaged over 50 disorder samples. In all the flat-band cases, $I(t)$ shows nontrivial behavior and keeps a non-vanishing value at $t = 2000$. On the other hand in the non-flat band cases, $I(t)$ decreases to zero rapidly.

LSA of the flat-band shows GUE-like behavior. Again, this behavior of $\langle \text{IPR} \rangle$ is an evidence of the crossover.

As our main concern is MBL in the flat-band, we studied the interacting cases with finite V 's. Calculations of the IPR for the case $V = 1$ are shown in in Fig. 2 (b). We find that the value of $\langle \text{IPR} \rangle$ of the flat-band increases in the weak disorder regime compared with the $V = 0$ case, and it again decreases considerably around $\mu \sim 6$ as in the $V = 0$ case. We investigated the cases other values of V , and found similar behavior of $\langle \text{IPR} \rangle$. We therefore conclude that *MBL exists in the flat-band Creutz ladder model in the weak disorder regime reflecting the flat-band structure, and crossover from the flat-band MBL to the strong-disorder MBL takes place as disorder is increased.* This is one of the main conclusions in this work.

Localization dynamics.— The above results of LSA and IPR indicate that disorder-free AL and MBL exist in the flat-band Creutz ladder. This motivates us to simulate dynamics of the Creutz ladder system. In the typical disorder-induced AL and MBL, information of an initial density-wave pattern is stored for a long period [3–6]. This behavior is a hallmark of ergodicity breaking, and indicates the breaking of eigenstate thermalization hypothesis [3, 39]. Here, we focus on the weak-disorder and disorder-free cases, and investigate whether the flat-band

Creutz ladder exhibits ergodicity breaking dynamics or not. To this end, we employ the Krylov subspace dynamical method [40, 41] and see how an initially prepared density-wave pattern evolves that is not entangled.

As a technical problem, the Lanczos algorithm for the temporal evolution of quantum states does not respect the orthogonality of the Krylov subspace vectors, and this causes deviations from the correct evolution of the system [11, 42]. To solve this problem, we employ the QR method [42] that preserves the orthogonality of the Krylov sub-space vectors in the time evolution [43].

We simulate the time evolution of the initial state such as $|\psi_{ini}\rangle = \sum_{i=1}^{L/4} a_{4i-3}^\dagger |0\rangle$. This density pattern is suitable for detecting localization dynamics as the Wannier state is localized over four sites in the flat-band regime as shown in Fig. 1 (a). As an indicator of ergodicity breaking dynamics, we introduce particle imbalance, $I(t)$, defined as

$$I(t) = \frac{N_o - N_e}{N_o + N_e}, \quad (4)$$

where $N_o \equiv \sum_{i=1}^{L/4} \sum_{\alpha=a,b} (n_{\alpha,4i-3} + n_{\alpha,4i-2})$ and $N_e \equiv \sum_{i=1}^{L/4} \sum_{\alpha=a,b} (n_{\alpha,4i-1} + n_{\alpha,4i})$. If the value of I is finite, memory of the initial state is preserved. This means ergodicity breaking. In the numerical calculation, we set unit of time by \hbar/t_1 , and use time slice $dt = 10^{-2}$. Figures 4 (a) and (b) show the time evolution of $I(t)$ in the disorder-free case ($\mu = 0$) for $L = 16$ and $L = 12$ with filling $1/8$, respectively. The results of $L = 16$ and $L = 12$ exhibit similar behaviors. For $V = 0$, the imbalance $I(t)$ for the flat-band keeps a finite value for long periods, while $I(t)$ for the non-flat-band immediately drops to zero. The above result indicates that the flat-band structure leads to a very slow relaxation of the initial state, and generates an ergodicity-breaking mechanism.

From Figs. 4 (a) and (b), it is obvious that the above behavior of $I(t)$ is preserved in the presence of the interaction. We conclude that the disorder-free MBL exists in the flat-band Creutz ladder with and without interactions, and *it has the ergodicity-breaking dynamics.*

We also calculated $I(t)$ for finite-disorder flat-band cases as shown in Fig. 4 (c). The result indicates that the disorder-free localization dynamics is robust against at least weak disorders. These behaviors are consistent with the results of the LSA in Fig. 2 and the IPR in Fig. 3. The finite value of I for a long period is related to Poisson-like distribution in the LSA and relatively large IPR compared to the AL of the non-flat-band. Results for the strong-disorder cases are given in Supplementary material [37].

Conclusion.— We clarified disorder-free AL and MBL phenomena induced by the flat-band structure in the Creutz ladder model with interactions. In the flat-band system, the LSA exhibits Poisson distribution in the weak-disorder regime for both free and interacting cases.

This result indicates the existence of the disorder-free AL and MBL phases in the Creutz ladder. We calculated the IPR that supports this result. Furthermore, we performed the dynamical simulations. We prepared a suitable density pattern as an initial state and simulated the system dynamics and measured the particle imbalance in the flat-band Creutz ladder. We found an ergodicity-breaking dynamics similar to that of the typical disorder-induced AL and MBL dynamics. This behavior is robust for weak disorders. Measurement of the particle imbalance is feasible in recent experiments [22, 24], and we hope that our findings will be confirmed in the near future. We also expect that phenomena similar to our findings will be observed in other kinds of flat-band models such as models on sawtooth lattice and Lieb lattice, which are to be realized by cold atoms [44, 45].

Acknowledgments.— Y. K. acknowledges the support of a Grant-in-Aid for JSPS Fellows (No.17J00486).

* These two authors contributed equally.

- [1] P. W. Anderson, *Phys. Rev.* **109** 1492 (1958).
- [2] A. Lagendijk, B. Van Tiggelen, and D. S. Wiersma, *Phys. Today* **62**, 24 (2009).
- [3] R. Nandkishore and D. A. Huse, *Annu. Rev. Condens. Matter Phys.* **6**, 15 (2015).
- [4] D. M. Basko, I. L. Aleiner, and B. L. Altshuler, *Ann. Phys.* **321**, 1126 (2006).
- [5] D. A. Abanin and Z. Papic, *Annalen der Physik* **529**, 1700169 (2017).
- [6] F. Alet and N. Laflorencie, *Comptes Rendus Physique* **19**, 498 (2018).
- [7] V. Oganesyan and D. A. Huse, *Phys. Rev. B* **75**, 155111 (2007).
- [8] M. Schreiber, S. S. Hodgman, P. Bordia, H. P. Luschen, M. H. Fischer, R. Vosk, E. Altman, U. Schneider, and I. Bloch, *Science* **349**, 842 (2015).
- [9] J.-Y. Choi, S. Hild, J. Zeiher, P. Schaus, A. Rubio-Abadal, T. Yefsah, V. Khemani, D. A. Huse, I. Bloch, and C. Gross, *Science* **352**, 1547 (2016).
- [10] S. Iyer, V. Oganesyan, G. Refael, and D. A. Huse, *Phys. Rev. B* **87**, 134202 (2013).
- [11] E. P. L. van Nieuwenburg, Y. Baum, and G. Refael, arXiv: 1808.00471 (2019).
- [12] M. Schulz, C. A. Hooley, R. Moessner, and F. Pollmann, *Phys. Rev. Lett.* **122**, 40606 (2019).
- [13] W. Li, A. Dhar, X. Deng, K. Kasamatsu, L. Barbiero, and L. Santos, arxiv: 1901.09762 (2019).
- [14] A. Smith, J. Knolle, D. L. Kovrizhin, and R. Moessner, *Phys. Rev. Lett.* **118**, 266601 (2017).
- [15] A. Smith, J. Knolle, R. Moessner, and D. L. Kovrizhin, *Phys. Rev. Lett.* **119**, 176601 (2017).
- [16] M. Brenes, M. Dalmonte, M. Heyl, and A. Scardicchio, *Phys. Rev. Lett.* **120**, 030601 (2018).
- [17] T. Takaishi, K. Sakakibara, I. Ichinose, and T. Matsui, *Phys. Rev. B* **98**, 184204 (2018).
- [18] A. Krishna, M. Ippoliti, and R. N. Bhatt, *Phys. Rev. B* **99**, 041111(R) (2019).
- [19] S. Takayoshi, H. Katsura, N. Watanabe, and H. Aoki, *Phys. Rev. A* **88**, 063613 (2013).
- [20] R. Mondaini, G. G. Batrouni, and B. Gremaud, *Phys. Rev. B* **98**, 155142 (2018).
- [21] M. Creutz, *Rev. Mod. Phys.* **73**, 119 (2001).
- [22] M. Mancini, G. Pagano, G. Cappellini, L. Livi, M. Rider, J. Catani, C. Sias, P. Zoller, M. Inguscio, M. Dalmonte, L. Fallani, *Science* **349**, 1510 (2015).
- [23] A. Celi, P. Massignan, J. Ruseckas, N. Goldman, I. B. Spielman, G. Juzeliunas, and M. Lewenstein, *Phys. Rev. Lett.* **112**, 043001 (2014).
- [24] J. H. Kang, H. Han, and Y. Shin, arXiv:1902.10304 (2019).
- [25] A. P. Schnyder, S. Ryu, A. Furusaki, and A. W. W. Ludwig, *Phys. Rev. B* **78**, 195125 (2008).
- [26] A. Kitaev, in *Advances in Theoretical Physics: Landau Memorial Conference*, edited by V. Lebedev and M. Feiguelfman, AIP Conf. Proc. No. 1134 (AIP, Melville, NY, 2009), p. 22.
- [27] L. F. Santos, and M. Rigol, *Phys. Rev. E* **81**, 036206 (2010).
- [28] E. Abrahams et al. *Phys. Rev. Lett.*, **42**, 673 (1979).
- [29] H. Grussbach, M. Schreiber, *Phys. Rev. B* **51**, 663 (1995).
- [30] S. Hikami, *Phys. Rev. B* **24**, 2671 (1981).
- [31] K. B. Efetov, A. I. Larkin, D. E. Khmel'nitsukii, *JETP* **52**, 568 (1980).
- [32] K. B. Efetov, "Supersymmetry in Disorder and Chaos", Cambridge Univ. Press (1977).
- [33] J. T. Chalker, T. S. Pickles, and P. Shukla, *Phys. Rev. B* **82**, 104209 (2010).
- [34] P. Shukla, *Phys. Rev. B* **98**, 184202 (2018).
- [35] The probability distribution is not a Gaussian orthogonal ensemble since our Hamiltonian matrix is not real-symmetric but only hermitian.
- [36] Similar recurrence phenomenon of glassy dynamics by disorder strength was observed recently for an extended Bose-Hubbard model, which is a quantum simulator of lattice gauge-Higgs model. J. Park, Y. Kuno, and I. Ichinose, arXiv: 1903.07297.
- [37] Supplementary material:
- [38] Small values of (IPR) is partly due to degeneracy coming from the translational symmetry of the model. For small disorder regime, the breakdown of the translational symmetry is weak. Accordingly, there exist a number of quasi-degenerate states.
- [39] P. Sierant and J. Zakrzewski, *New J. Phys.* **20**, 043032 (2018).
- [40] P. Prelovsek, J. Bonca, *Strongly Correlated Systems: Numerical Methods*, vol. 176, Springer, 2013.
- [41] S. R. Manmana, A. Muramatsu, and R. M. Noack, AIP Conf. Proc. **789**, 269 (2005).
- [42] N. Mohankumar and S. M. Auerbach, *Comput. Phys. Commun.* **175**, 473 (2006).
- [43] We thank the authors of ref [11] for the release of their code on the GitHub, which was used in [11].
- [44] T. Zhang and G.-B. Jo, *Scientific Reports* **5**, 16044 (2015).
- [45] S. Taie, H. Ozawa, T. Ichinose, T. Nishio, S. Nakajima, and Y. Takahashi, *Sci. Adv.* **1** (2015), 10.1126/sciadv.1500854.

Supplemental Material

I. System-size dependence in level spacing analysis

In the level spacing analysis (LSA), the results depends slightly on system size. In our numerical simulation, the system size is limited up to $L = 16$, and $N = 4$ (filling $1/8$ case). In the LSA, as mentioned in the main text, we employ the unfolding method to obtain a clear probability distribution. As a concrete example, we show the system-size dependence for non-interacting flat-band case in Fig .A1 (a). For $L = 8$ case, the shape of the probability distribution is apart from Poisson distribution. The value of $P(s)$ around $s \sim 0$ tends to increase for small system size. As increasing the system size up to the $L = 16$, the shape of the probability distribution seems fairly close to Poisson. From this tendency, we expect that on calculating for larger system sizes, the probability distribution approaches to the exact Poisson distribution. Therefore for the non-interacting flat-band system, the AL is expected to be clearly observed in a large system size. Such a system-size dependence exists also for the interacting case. Figure A1 (b) shows the system-size dependence of the LSA for $V = 1$ case. Compared with the non-interacting case, increasing tendency of $P(s)$ in the vicinity of $s \sim 0$ in the small systems is weak. However, the probability distribution deviates from the exact Poisson distribution. As increasing the system size up to the $L = 16$, the probability distribution approaches to the Poisson distribution.

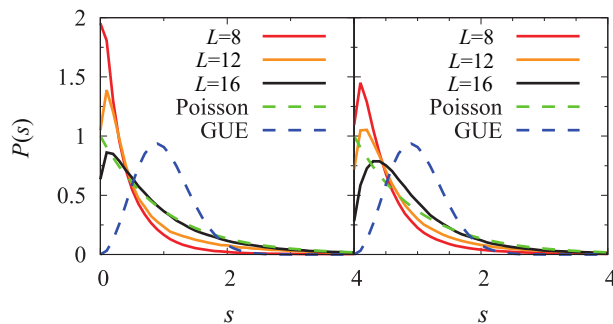


FIG. A1: System-size dependence of level spacing analysis: (a) non-interacting flat band case with $\mu = 1$. (b) interacting flat band case with $\mu = 1$. In both cases, the level spacing distribution, $P(s)$, approaches to the Poisson distribution as the system size is increased.

II. Dynamical properties of the Creutz ladder with strong disorders

As shown in Fig. 4 (c) in the main text, we studied the time evolution of the density-wave type configuration in the weak-disorder regime $\mu \leq 1$. Here, we consider the strong-disorder regime of the interacting flat-band case.

As shown in the calculations of the LSA and IPR in the main text, the GUE-like behavior appears for moderate disorder strength such as $\mu \sim 6$. For the stronger disorder regime, the probability distribution in the LSA returns to the Poisson distribution, where the ordinary disorder-induced AL or MBL is expected to occur. By using the Krylov subspace method explained in the main text, we calculated the dynamics of the particle Imbalance, $I(t)$, defined as Eq. (4) in the main text. Figure A2 shows the results of time evolution of $I(t)$ in the strong-disorder system with $V = 1$ for $L = 12$, $N = 3$. The results are in good agreement with the LSA and the IPR obtained in the main text. For $\mu = 6$ case, the LSA exhibits the GUE-like distribution probability. Here, calculation of $\mu = 6$ in Fig. A2 shows that $I(t)$ decreases to a vanishingly small value in a long time evolution. On the other hand, the $\mu = 30$ result indicates that the particle imbalance remains finite even in a long time evolution. This behavior is the typical MBL dynamics induced by disorder and consistent to the results of both the LSA and IPR calculations.

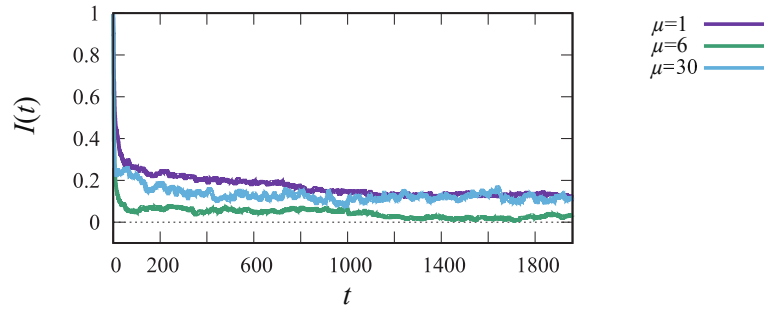


FIG. A2: Time evolution of Imbalance, $I(t)$, for $\mu = 1, 6$ and 30 in the flat-band system with $V = 1$. Interestingly enough, $I(t)$ for $\mu = 6$ decreases to a vanishingly small value, whereas $I(t)$ for $\mu = 6$ and 30 keeps a finite value. This behavior is in good agreement with the results of the LSA and IPR, which indicate the existence of the crossover at $\mu \sim 6$. $L = 12$, $N = 3$. We averaged calculations over 50 disorder samples.